A SCHEME FOR PUMP-PROBE EXPERIMENTS AT X-RAY SASE FEL*

E.L. Saldin, E.A. Schneidmiller, and M.V. Yurkov
Deutsches Elektronen-Synchrotron (DESY), Hamburg, Germany

Abstract

We propose a new scheme for two-color operation of an X-ray Self-Amplified Spontaneous Emission Free Electron Laser. The scheme is based on an intrinsic feature of such a device: chaotic modulations of electron beam energy and energy spread on the scale of FEL coherence length are converted into large density modulations on the same scale with the help of a dispersion section, installed behind the x-ray undulator. Powerful radiation is then generated with the help of a dedicated radiator (like an undulator that selects a narrow spectral line), or one can simply use, for instance, broadband edge radiation. Typical radiation wavelength can be as short as FEL coherence length, and can be red-shifted by increasing the dispersion section strength. In practice it means the wavelength range from vacuum ultraviolet to infrared. The long-wavelength radiation pulse is naturally synchronized with x-ray pulse and can be either directly used in pump-probe experiments or cross-correlated with high power pulse from a conventional laser system. In this way experimenters overcome jitter problems and can perform pump-probe experiments with femtosecond resolution. The proposed scheme is very simple, cheap and robust, and can be easily realized in facilities like FLASH, European XFEL, LCLS, and SCSS.

INTRODUCTION

Free-electron lasing at wavelengths shorter than the ultraviolet can be achieved with a single-pass, high-gain FEL amplifier [1]. Due to lack of powerful, coherent seeding sources, short-wavelength FEL amplifiers work in the so called Self-Amplified Spontaneous Emission (SASE) mode, where the amplification process starts from shot noise in the electron beam [2, 3, 4]. Present acceleration and FEL techniques allow to generate powerful, coherent femtosecond pulses in wavelength range from vacuum ultraviolet (VUV) [5, 6, 7] through soft X-ray [8, 9] to hard X-ray [10].

There is a growing interest among FEL users in pump-probe experiments with femtosecond resolution, extended into X-ray regime [11, 12, 13]. However, synchronization of pulses from an X-ray FEL with optical pulses from a conventional laser with femtosecond accuracy is not a trivial task due to a jitter in an electron bunch arrival time. The most simple and reliable way to get around this obstacle is to produce an X-ray pulse and a long-wavelength radiation pulse by the same electron bunch [14, 15]. If the optical pulse is sufficiently powerful, it can be directly used in a pump-probe experiment. Otherwise this long-wavelength radiation pulse can be used for cross-correlation measurement with a powerful pulse from a conventional laser (that is used in pump-probe experiment) [17]. This allows one to determine a relative delay between two pulses for every shot and then to sort out experimental data using this information. Different scenarios were considered [14, 15, 16, 17, 18] for producing visible or infrared radiation by the same electron bunch that lases in X-ray undulator. Here we propose very cheap and robust method, based on natural features of a SASE FEL.

EFFECT DESCRIPTION

SASE FEL is a high-gain FEL amplifier starting up from shot noise in electron beam. The properties of such a device are described in details in [1]. On top of density and energy modulations in the electron beam on the scale of a resonant wavelength λ_r, there are long-scale envelope modulations. The latter modulations have a typical scale of FEL coherent length, $l_c \simeq \lambda_r/(2\pi\rho)$, where ρ is the well-known FEL parameter [19]. However, there are no spectral components of density modulation in the range $\lambda \simeq l_c$ (more precisely, there can be small modulations of the order of ρ when SASE FEL reaches saturation). Here we propose a simple trick which can be used in order to get large density modulations of the order of one.

Let us consider a continuous electron beam of which longitudinal phase space at the exit of FEL undulator can be described by a distribution function $f(P, s)$, where $P = \mathcal{E}-\mathcal{E}_0$ is energy deviation from a nominal value, and s is the coordinate along the bunch. It is convenient to use scaled variables $\hat{P} = \rho P/\mathcal{E}_0$ and $\hat{s} = \rho k_r s$, where $k_r = 2\pi/\lambda_r$. Before FEL interaction we assume the function $f(\hat{P}, \hat{s})$ to be independent of $\hat{s}$, i.e. to have distribution in $\hat{P}$ with the rms width $\hat{\Lambda}_T$ which is constant along the beam. In the following we will assume that $\hat{\Lambda}_T \ll 1$ since it is usually the case. The distribution function is normalized such that after integration over $\hat{P}$ one gets unity for unmodulated beam case. FEL process modifies the distribution function as it was noticed above: there are energy and density modulations on the scale of λ_r with a chaotically changing envelope on the scale of l_c (i.e. when $\Delta\hat{s} \simeq 1$). Note that FEL induced energy modulation and mean energy loss are typically $\hat{P} \simeq 1$ at saturation and $\hat{P} \ll 1$ in the exponential gain regime before saturation.

Let us install behind SASE undulator a dispersive element (like a simple four-bend chicane) with longitudinal dispersion characterized by matrix element R_{56}. After beam passes the dispersive section, a particle's co-

* FEL 2009 Conference, WEPC48

ordinate changes such that one should use the substitution $s \rightarrow s - R_{56}P/\mathcal{E}_0$ in the distribution function. In scaled variables this would read $f(\hat{P}, \hat{s} - \hat{P}\hat{R}_{56})$, where $\hat{R}_{56} = \rho^2 k_r R_{56}$. Even a relatively small strength of the dispersion section is sufficient to completely smear small-scale modulations due to the energy spread. The condition for that can be formulated as $\hat{\Lambda}_T \hat{R}_{56} \gg \rho$, and it will always be fulfilled in the rest of the paper. Therefore, after dispersion section we only deal with large-scale modulations. Let us first consider the case when $\hat{R}_{56} \ll 1$. In this case the distribution function can be expanded as follows:

$$f(\hat{P}, \hat{s} - \hat{P}\hat{R}_{56}) \simeq f(\hat{P}, \hat{s}) - \frac{\partial f}{\partial \hat{s}} \hat{P}\hat{R}_{56} + \frac{1}{2}\frac{\partial^2 f}{\partial \hat{s}^2}\hat{P}^2\hat{R}_{56}^2 + ...$$

Note that the distribution function before the dispersion section is differentiated here, but the small-scale modulations are assumed to be smeared as discussed above. Integrating over $\hat{P}$ (and exchanging differentiation and integration) we get current modulation

$$I/I_0 \simeq 1 - \hat{R}_{56}\frac{\partial}{\partial \hat{s}} \int \hat{P} f d\hat{P} + \frac{\hat{R}_{56}^2}{2}\frac{\partial^2}{\partial \hat{s}^2} \int \hat{P}^2 f d\hat{P} + ...$$

which can be rewritten as

$$I/I_0 \simeq 1 - \hat{R}_{56}\frac{\partial < \hat{P} >}{\partial \hat{s}} + \frac{\hat{R}_{56}^2}{2}\frac{\partial^2 < \hat{P}^2 >}{\partial \hat{s}^2} + ... \quad (1)$$

A leading term here is connected with the derivative of beam energy loss due to SASE process. The second term depends on induced rms energy spread and mean energy loss. At saturation $< \hat{P} >$ and $< \hat{P}^2 >$ are typically of the order of one, they change on a typical scale $\Delta\hat{s} \simeq 1$, so that current modulation is of the order of $\hat{R}_{56}$. Although Eq. (1) is not valid when $\hat{R}_{56} \simeq 1$, one can extrapolate the tendency and estimate that in this case one can reach very strong current modulation, on the order of one. This is confirmed by numerical simulations performed with 1-D version of the code FAST [20]. One can also notice that for small values of $\hat{R}_{56}$ the current modulation pattern remains unchanged while its amplitude linearly increases with $\hat{R}_{56}$. When $\hat{R}_{56} \simeq 1$ the pattern is modified due to high-order terms, some red shift of the modulation spectrum can be observed. When $\hat{\Lambda}_T \hat{R}_{56} \simeq 1$ the high-frequency components of current modulation (that appeared at low $\hat{R}_{56}$) are smeared, and the spectrum of the modulation is strongly red-shifted. This tendency is illustrated in the next Section.

APPLICATION TO EUROPEAN XFEL

Let us consider a possible operation of long-wavelength afterburner behind SASE1 undulator of the European XFEL. To be specific, we assume that it operates at 0.1 nm. Parameters of the electron beam, undulator, and FEL radiation can be found in [13]. The simulations of the FEL process were performed with 3-dimensional, time-dependent code FAST [20]. Then particles' positions in the bunch

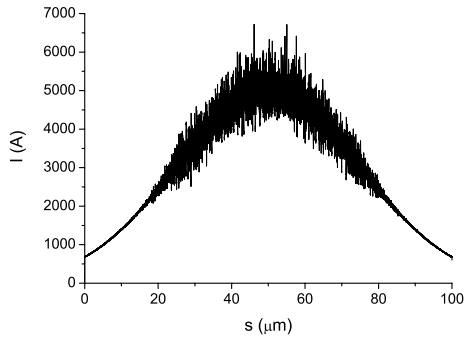

Figure 1: Modulation of current in the beam passed SASE1 undulator [13] and a dispersion section with R_{56} equal to 50 μm.

were changed in accordance with their energies and applied R_{56}. Parameter ρ in the considered case is equal to 4×10^{-4}. Thus, it is easy to calculate that parameter $R_{56} = 100$ μm corresponds to the scaled parameter $\hat{R}_{56} = 1$. As a technical realization of dispersion section for XFEL we consider a simple and compact 4-bend chicane. In Fig. 1 and Fig. 2 (left plot) one can see chaotic modulations of the beam current for the case when R_{56} dispersion section is equal to 50 μm. For smaller values of the R_{56} the pattern remains the same but the amplitude reduces proportionally. For larger values of the R_{56} the pattern gets strongly modified as one can see from Fig. 2, the modulations have longer scale. Figs. 1,2 are calculated for a given shot. It is worth mentioning that the pattern would change shot-to-shot since SASE is stochastic process.

In Fig. 3 we present ensemble average modulus of the bunch form factor $|F(\lambda)|$ (Fourier transform of the bunch profile). This is a useful notion because energy spectral density of radiation produced by a bunch in any radiator is given by

$$p(\lambda) = p_1(\lambda)\left[N_e + N_e(N_e - 1)|F(\lambda)|^2\right] , \quad (2)$$

where $p_1(\lambda)$ is the energy spectral density produced by a single electron, and N_e is the number of electrons in the bunch. Linear in N_e term gives usual incoherent radiation (spontaneous emission). Thus, a modulated bunch radiates by a factor $N_e|F(\lambda)|^2$ more energy at a given wavelength than an unmodulated bunch. Here we consider the bunch with the charge of 1 nC ($N_e = 6.2 \times 10^9$) so that one can expect an enhancement over spontaneous emission by a factor up to 4×10^4, using $|F(\lambda)|$ from Fig. 3.

One should not be surprised by the fact that the amplitude of modulations in Figs. 1,2 is typically 10-20 %, while the form-factor is smaller by almost 2 orders of magnitude. For a monochromatic modulation the value of form-factor would indeed have been of the order of 0.1. Chaotic spikes, however, add randomly to the Fourier transform and the result is suppressed roughly by square root of number of spikes, and the spectrum is broad-band. One should also

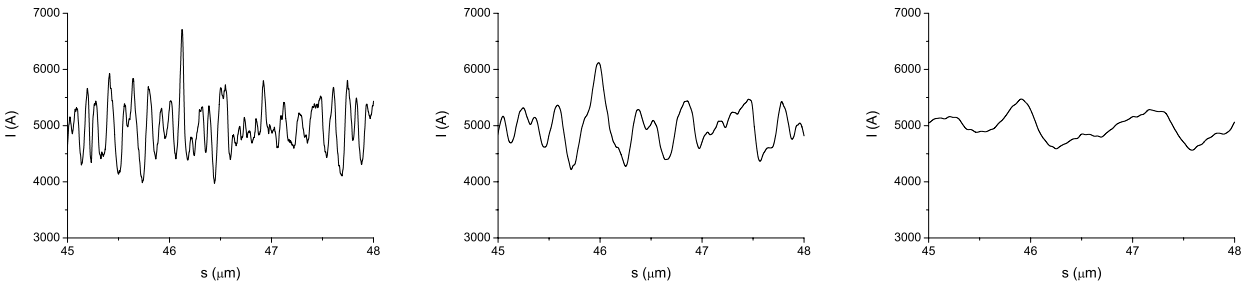

Figure 2: Modulation of current in the beam passed SASE1 undulator and a dispersion section with R_{56} equal to 50 μm (upper plot, enlarged fraction of Fig. 1), 200 μm (middle plot), and 500 μm (lower plot).

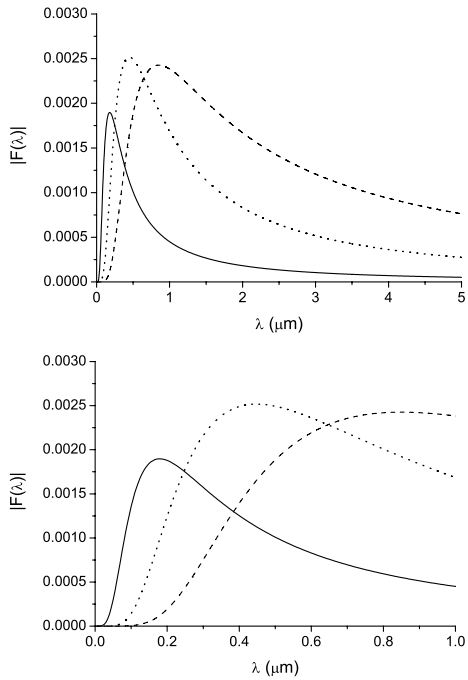

Figure 3: Ensemble average modulus of the bunch form factor versus wavelength for SASE1 afterburner, and an enlarged fraction of this plot, for the R_{56} of the dispersion section equal to 50 μm (solid), 200 μm (dot), and 500 μm (dash).

note here that a single shot form factor are also chaotically modulated, while the smooth curves in Fig. 3 are the results of statistical averaging.

Form factor for different values of R_{56} is presented in Fig. 3. For $R_{56} = 50$ μm the high-frequency cut-off is at the wavelength about 100 nm which coincides with the coherence length of SASE FEL operating at 0.1 nm (note that one can have a significant enhancement over spontaneous emission even at 40-50 nm). For larger values of the R_{56} one can observe a red shift. Thus, by varying R_{56} one can easily optimize form factor in the wavelength range from VUV to infrared. Let us now discuss how to produce radiation that can be transported to experimental hall and used in

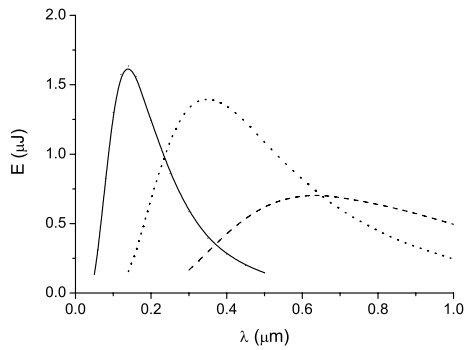

Figure 4: Radiation pulse energy within a central cone of the SASE1 afterburner undulator versus wavelength for the R_{56} of the dispersion section equal to 50 μm (solid), 200 μm (dot), and 500 μm (dash).

pump-probe experiments as described in [17]. In principle, one can make use of edge radiation as described in [17]. In that case a broad-band radiation would be produced (which can be then filtered if necessary). We consider here an alternative radiator, namely a long-period undulator (similar to that installed in FLASH [21]). Let us consider as an example, a ten-period undulator with a period length 70 cm and a maximum field 12 kGs. For the electron energy 17.5 GeV one can tune resonant wavelength between 50 nm and 1 μm. To calculate radiation pulse energy one should use the fact that in a planar undulator with large K-value 0.011 photons per electron is radiated spontaneously within a central cone (given by $\sqrt{\lambda/L_w}$, where L_w is the undulator length). Then, using Eq. (2) and Fig. 3 we end up with the Fig. 4 from which we see that pulse energies are in μJ range within a central cone and with spectral bandwidth 10%. Estimated shot-to-shot fluctuations will be below 10%. Note that similar long-wavelength afterburners can be installed behind other SASE undulators, in particular after SASE3.

APPLICATION TO FLASH

FLASH is the SASE FEL operated as the user facility in the wavelength range 6.5-50 nm [6, 8, 9]. There is nine-

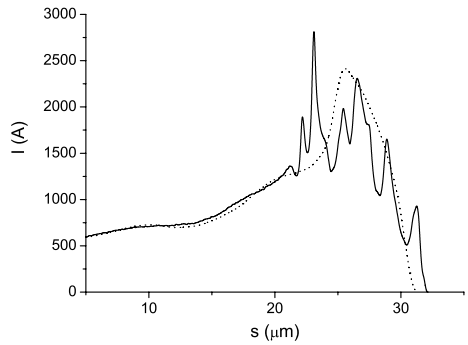

Figure 5: Modulation of current in the head of electron bunch lasing at 7 nm in VUV undulator of FLASH and passing FIR undulator with R_{56} equal to 250 μm (solid), and with $R_{56} = 0$ (dots). Only small part of the bunch is shown, bunch head is on the right

period FIR (far infrared) undulator [21] installed behind the main SASE undulator. Its wavelength range spans from sub-μm up to 200 μm. The R_{56} of an undulator is given by a simple formula: $R_{56} = 2N_w\lambda_r$, where N_w is the number of periods and λ_r is the resonant wavelength. Thus, the R_{56} of this undulator can be tuned from 0 to a few mm, and it can serve in the considered scheme as a dispersive section and a radiator (radiating at higher harmonics) at the same time. In addition, edge radiation can be produced behind this undulator (there is a few m drift between the undulator and the beam dump, so that there is enough space for formation of such radiation in visible and near-infrared range). We illustrate with a numerical example a possible operation of afterburner. We consider lasing at 7 nm and use in simulations an electron beam with the parameters close to those used in [8] but rescaled to 1 GeV. The bunch with the charge of 0.5 nC consists of a few ps long low-current tail and a short high-current leading peak (shown in Fig. 5 in dots) that produces FEL radiation. We illustrate conversion of FEL-induced energy modulations to modulations of beam current by applying the $R_{56} = 250\ \mu m$ (which corresponds to tuning of FIR undulator to 14 μm resonant wavelength). In Fig. 5 one can see a realization of such modulations in time domain, and Fig. 6 shows form factor, corresponding to this specific shot. Note that form factor of undisturbed bunch decays at 5-10 μm, and the effect, described in this paper, allows one to extend the possibility to produce powerful radiation to 1 μm and below [1]. For instance, in a given example the radiation in the range 0.7-1 μm would be about 4 orders of magnitude above spontaneous emission level.

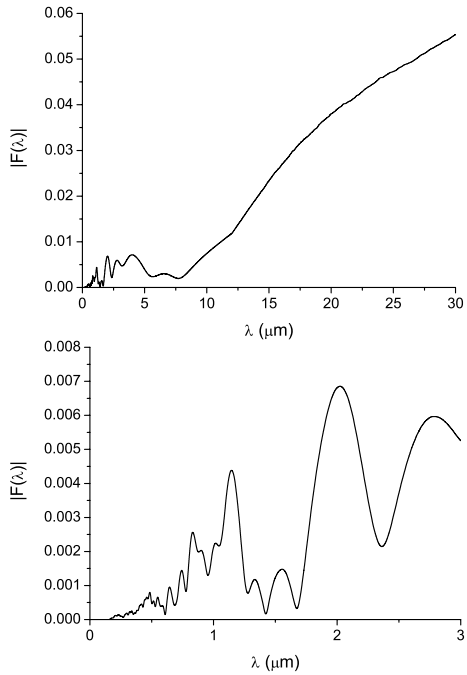

Figure 6: Modulus of the bunch form factor (corresponding to realization in time domain shown in Fig. 5) versus wavelength, and an enlarged fraction of this plot.

REFERENCES

[1] E.L. Saldin, E.A. Schneidmiller and M.V. Yurkov, "The Physics of Free Electron Lasers", Springer, Berlin, 2000.

[2] A.M. Kondratenko and E.L. Saldin, Part. Accelerators **10**(1980)207.

[3] Ya.S. Derbenev, A.M. Kondratenko and E.L. Saldin, Nucl. Instrum. and Methods **193**(1982)415.

[4] J.B. Murphy and C. Pellegrini, Nucl. Instrum. and Methods A **237**(1985)159.

[5] V. Ayvazyan et al., Phys. Rev. Lett. **88**(2002)104802.

[6] V. Ayvazyan et al., Eur. Phys. J. **D37**(2006)297.

[7] T. Shintake et al., Nature Photonics **2**(2008)555.

[8] W. Ackermann et al., Nature Photonics **1**(2007)336.

[9] K. Tiedtke et al., New Journal of Physics **11**(2009)023029.

[10] P. Emma, "First lasing of the LCLS X-ray FEL at 1.5 A", presented at the Particle Accelerator Conf., Vancouver, May 2009.

[11] J. Arthur et al., Linac Coherent Light Source (LCLS). Conceptual Design Report, SLAC- R593, Stanford, 2002 (see also http://www-ssrl.slac.stanford.edu/lcls/cdr.

[12] SCSS X-FEL: Conceptual design report, RIKEN, Japan, May 2005. (see also http://www-xfel.spring8.or.jp).

[13] M. Altarelli et al. (Eds.), XFEL: The European X-Ray Free-Electron Laser. Technical Design Report, Preprint DESY 2006-097, DESY, Hamburg, 2006 (see also http://xfel.desy.de).

[14] B. Faatz et al., Nucl. Instrum. and Methods **A 475**(2001)363.

[15] J. Feldhaus et al., Nucl. Instrum. and Methods **A 528**(2004)453.

[16] A. Zholents and W.M. Fawley, Phys. Rev. Lett. **92**(2004)224801.

[17] G.A. Geloni et al., Opt. Commun. **281**(2008)3762.

[18] E.L. Saldin, E.A. Schneidmiller and M.V. Yurkov, Proc. of 29th FEL Conf. (2007), p. 248.

[19] R. Bonifacio, C. Pellegrini and L.M. Narducci, Opt. Comm. **50**(1984)373.

[20] E.L. Saldin, E.A. Schneidmiller and M.V. Yurkov, Nucl. Instrum. and Methods **A 429**(1999)233.

[21] Gensch et al., Infrared Physics & Technology, 51 (2008) 423.

[1] Note that some observations of such kind were done at FLASH, and now we can hope for systematic studies.